European Journal of Radiology 180 (2024) 111668

Contents lists available at ScienceDirect

European Journal of Radiology

journal homepage: www.elsevier.com/locate/ejrad

An exploration of radiological signs in post-intervention liver complications

Faezeh Khorasanizadeh [a,1], Narges Azizi [a,1], Roberto Cannella [b,*], Giuseppe Brancatelli [b]

[a] Advanced Diagnostic and Interventional Radiology Research Center (ADIR), Tehran University of Medical Science, Tehran, Iran
[b] Section of Radiology - Department of Biomedicine, Neuroscience and Advanced Diagnostics (BiND), University of Palermo, Palermo, Italy

ARTICLE INFO

Keywords:
Hepatobiliary interventions
Computed tomography
Magnetic resonance imaging
Ultrasound

ABSTRACT

The advent and progression of radiological techniques in the past few decades have revolutionized the diagnostic and therapeutic landscape for liver diseases. These minimally invasive interventions, ranging from biopsies to complex therapeutic procedures like transjugular intrahepatic portosystemic shunt placement and transarterial embolization, offer substantial benefits for the treatment of patients with liver diseases. They provide accurate tissue diagnosis, allow real-time visualization, and render targeted treatment for hepatic lesions with enhanced precision. Despite their advantages, these procedures are not without risks, with the potential for complications that can significantly impact patient outcomes. It is imperative for radiologists to recognize the signs of these complications promptly to mitigate further health deterioration. Ultrasound, CT, and MRI are widely utilized examinations for monitoring the complications. This article presents an overarching review of the most commonly encountered hepatobiliary complications post-radiological interventions, emphasizing their imaging characteristics to improve patient post-procedure management.

1. Introduction

In recent decades, radiological interventions have played an increasingly important role in the diagnosis and management of a range of liver diseases [1]. These interventions with numerous benefits, from enabling accurate tissue diagnosis to providing therapeutic solutions for hepatic parenchymal diseases and hepatic tumors, have emerged as vital tools for clinicians [2,3]. Radiological approaches not only offer less invasive alternatives to traditional surgical methods but also facilitate real-time visualization, which can enhance precision and optimize outcomes [4,5]. Each intervention, be it biopsy, open or laparoscopic liver resection, open or laparoscopic cholecystectomy, percutaneous cholecystostomy, transjugular intrahepatic portosystemic shunt (TIPS), chemical ablation, thermal ablation, newer ablative techniques such as irreversible electroporation, transcatheter arterial treatments including transarterial embolization, chemoembolization (TACE), or radioembolization, has brought about its indication and procedural imaging characteristics [6–11]. However, all these procedures carry a potential risk of several complications [12–14]. These complications necessitate close monitoring and a nuanced understanding of radiological results to ensure optimal patient outcomes. Fig. 1 presents a comprehensive summary of the most common hepatobiliary complications observed post-intervention.

Due to the wide variety of complications and their serious effects on patient outcomes, understanding the imaging signs of these complications is crucial. Table 1 delineates the most prevalent hepatobiliary complications associated with common liver interventions, including their frequencies. Recognizing the radiological features of these post-intervention complications is essential to improve the management of such conditions, mitigating further clinical deterioration. Our article aims to comprehensively review the key radiological features of common hepatobiliary complications, including infectious, biliary, and hemorrhagic types. This will provide a detailed visual guide, aiding radiologists in accurately identifying and addressing these complications following liver interventions.

2. Abscess formation

Hepatic abscesses, although not common, are complications within-hospital mortality of 9.6 % [59]. These abscesses manifest post-intervention, with symptoms ranging from fever, chills, malaise, and abdominal discomfort to elevated white blood cell [60]. Several risk

* Corresponding author at: Department of Biomedicine, Neuroscience and Advanced Diagnostics (BiND), University of Palermo, Via del Vespro 129, Palermo 90127, Italy.
E-mail address: roberto.cannella@unipa.it (R. Cannella).
[1] These authors contributed equally.

https://doi.org/10.1016/j.ejrad.2024.111668
Received 9 April 2024; Received in revised form 28 July 2024; Accepted 2 August 2024
Available online 5 August 2024

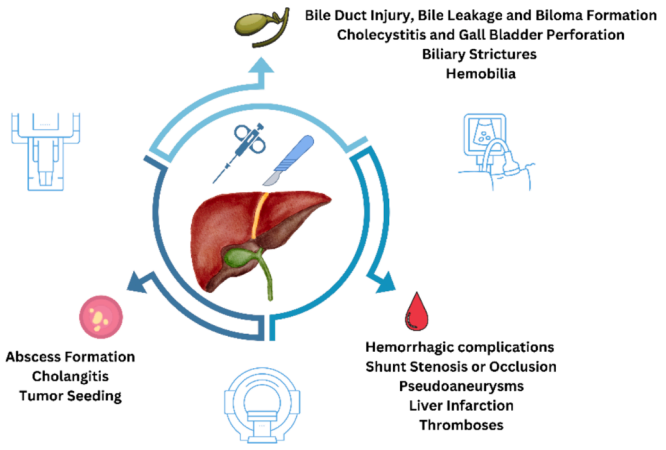

Fig. 1. The perspective of post-intervention liver complications.

factors predispose individuals to the formation of hepatic abscesses: pre-existing biliary-enteric anastomosis, external drainage, malfunctioning Oddi sphincter, underlying diabetes mellitus, and residual iodized oil from prior TACE procedures [61]. The compromised function of the duodenal extensor muscle can heighten the risk, as it predisposes the bile ducts to bacterial influx from the bowel lumen [62,63].

Imaging has a crucial role in the characterization, differential diagnosis, and extension of patients with suspected hepatic abscess. Ultrasonography (US) typically reveals these abscesses as hypoechoic, circumscribed lesions, or larger heterogeneous masses with internal septa and hyperechoic cellular debris. This method detects lesions over 2 cm with 85–95 % sensitivity [64]. Notably, color Doppler examination often demonstrates an absence of central vascularization [65]. When utilizing contrast-enhanced ultrasonography (CEUS), the abscess is discerned as a lesion with heterogeneous peripheral enhancement, delineated by a hypoechoic center, an echoic rim, and thin vessels tracing the septa and boundaries [66]. On computed tomography (CT), hepatic abscesses typically appear as hypodense lesions, which can be either isolated or confluent. This modality demonstrates a 95 % sensitivity in identifying abscesses as small as 0.5 cm [64]. Contrast-enhanced CT can demonstrate a central hypodense fluid area encased by a vivid hyperdense rim and an outer hypodense halo—known as "double-target" appearance. The inner rim corresponds to the abscess wall and exhibits sustained enhancement, while the external one corresponds to the liver parenchyma, showing delayed phase enhancement [67]. Additionally, a cluster sign — defined as a concentrated aggregation of numerous small (<2cm) low-density lesions within the liver — indicates an early stage in the formation of pyogenic abscesses [68]. Rarely, the sporadic presence of air microbubbles within the abscess can be observed (Fig. 2) [67]. Magnetic Resonance Imaging (MRI) can demonstrate a T1-hypointense and T2-hyperintense lesion, with sensitivity of 100 % and specificity of 96.3 %. High signal intensity in diffusion weighted images (DWI) combined with low signal intensity on apparent diffusion coefficient (ADC) can be leveraged to guide precise drainage in instances of multiple collections [69].

Differentiating hepatic abscesses, tumor necrosis, liver infarction, and secondary infection after TACE is challenging. Liver infarctions appear as well-defined, hypodense, wedge-shaped lesions from the hilum to the capsule, resulting from reduced blood flow or blocked vessels. Tumor necrosis in the liver manifests as non-enhancing areas in tumors on contrast-enhanced scans, typically due to insufficient blood supply, contrasting with infarctions' usually with irregular boundaries. Additionally, secondary infection in infarctions showed interval rounding and sometimes developed internal foci of gas, which is indicative of infection. The internal gas formation appeared focally localized with a mottled appearance or an air–fluid level, different from the linear branching pattern of pneumobilia [63]. Hemostatic material, used to stop bleeding during open surgeries, also presents a differential diagnosis challenge for abscesses. To distinguish, it's crucial to know the patient's surgical history and consult with the surgeon regarding the use of hemostatic material. Unlike abscesses, gas pockets in hemostatic material usually form straight lines without showing gas-fluid levels. While rim enhancement is typically absent, a granulomatous reaction around the material may induce it after several days surrounded by a robust peripheral enhancement [60].

Differentiating expected post-ablation findings from hepatic abscess formation is also crucial for appropriate patient management. Post-ablation changes typically include an ablation zone characterized by hypodensity on CT, which may show rim-like enhancement due to reactive hyperemia and central hyperdense areas from cellular disruption [70]. Small air bubbles could be seen immediately post-ablation due to tissue fluid boiling but usually resolve by the first or second follow-up [70]. In contrast, hepatic abscess formation is suggested by interval enlargement of the ablation zone, persistent or new air-fluid levels, and clinical signs of infection [70,71]. Additionally, DWI has demonstrated its utility in distinguishing between infected and non-infected collections [72].

3. Cholangitis

Cholangitis after hepatobiliary procedures, as an inflammation of the bile duct, presents a critical risk with a mortality rate between 2 % to 4.5 %, often due to anastomosis stenosis following surgery [73–75]. However, it might occur following minimal invasive interventions such as transhepatic biliary drainage, biliary stent placement, or percutaneous transhepatic cholangiography [76]. The importance of recognizing this condition lies in its potential to lead to serious complications, including biliary sepsis, liver abscesses, and in severe cases, multiorgan failure if not promptly addressed [75,77,78].

The imaging features of post-hepatic intervention cholangitis can be subtle and require a high index of suspicion [79]. On US, findings indicative of cholangitis might include biliary wall thickening and pericholedochal echogenicity signaling inflammation. While the US shows sensitivity of 73 % for detecting choledocholithiasis, it has lower sensitivity for other obstructive pathologies [80,81]. It's critical to recognize that a normal US does not rule out cholangitis, prompting the need for additional imaging modalities [80]. CT imaging without contrast may reveal nonspecific biliary dilation. However, post-contrast CT can show enhancement of the bile duct walls, periductal enhancement representing inflammation, and may also identify complications such as abscesses or leaked bile, with both sensitivity and specificity exceeding 83 %. This modality is also adept at identifying emergent complications, including abscess formation [82]. MRI, particularly with MR cholangiopancreatography (MRCP), with sensitivity of 96 % and specificity of 100 %, is the most sensitive modality for detecting biliary abnormalities [83]. It can delineate the biliary tree in detail and, with contrast, can highlight areas of inflammation and infection, differentiating from fibrosis and malignancy. [83].

4. Biloma

Biliary complications such as bile duct injury, bile leakage and biloma are uncommon after intervention, but any delay in their diagnosis and treatment can lead to severe, life-threatening consequences [84]. Bile leakage can result in the formation of bilomas, which are defined as any well-circumscribed intra-abdominal bile collections, either encapsulated or non-encapsulated, external to the biliary tree [85]. The disruption of the biliary tree, often due to iatrogenic injury or abdominal trauma, can lead to either intrahepatic or extrahepatic biloma formation. Bilomas can exacerbate the prognosis of hepatic abscesses and are linked to significant morbidity and mortality if not promptly diagnosed and managed appropriately [86]. The clinical presentation of bilomas can be variable and often subtle, making

Table 1
The most common liver interventions, the most prevalent hepatobiliary complications, and their reported frequency.

Procedure	The most common hepatic complications	Reported frequency (%)	Reference
Liver Biopsy	Hemorrhagic complications	0.11–10.9	[15,16]
	Bile peritonitis	0.03–0.22	[17]
	Hemobilia	0.01–0.20	[16]
	Hemoperitoneum	0.03–0.70	[17]
	Biopsy of surrounding organs	0.00–0.04	[17]
	Arteriovenous fistula	5.40	[17,18]
	Breakage of the biopsy instrument	0.02–0.06	[17]
Liver Resection	Hemorrhagic complications	1.96–5.96	[19,20]
	Bile leakage	1.35–19.61	[19]
	Biloma	0.98	[19]
	Perihepatic abscess	0.98–3.02	[19,21]
	Cholangitis	0.98	[19]
	Portal vein thrombosis	1.57–20.00	[22,23]
	Liver failure	0.68–2.80	[21]
Cholecystectomy	Hemorrhagic complications	0.59–3.64	[24]
	Bile leakage/fistula	0.59–21.05	[25]
	Biloma	2.50*	[26]
	Biliary strictures	0.00–0.89	[27]
	Retained gallstones	0.40–4.17	[24,28]
	Subhepatic collection	7.14–10.53	[25,28]
	Pseudoaneurysms	N/A**	
Percutaneous Cholecystostomy	Hemorrhagic complications	1.65–3.55	[29,30]
	Biloma/Abscess formation	0.41	[29]
	Catheter blockage	8.89	[31]
	Catheter leakage	4.44	[31]
	Catheter dislodgement	0.03–4.54	[29,31]
Ablation	Hemorrhagic complications	0.52–14.51	[32]
	Thermal biliary injuries or stenosis***	0–10.5	[13]
	Irreversible electroporation biliary injuries	1.80	[33]
	Biloma	0.04–0.20	[32,34]
	Biliary stricture	0.04–0.22	[32]
	Cholecystitis	0.04–3.23	[32]
	Cholangitis	1.46	[35]
	Abscess formation	0.26–4.71	[32,33,36]
	Tumor Seeding	0.00–0.52	[32,37]
	Portobiliary fistula/Hemobilia	0.04–0.48	[32]
	Arterioportal fistula	0.08–0.39	[32,38]
	Thrombosis of portal vein	0.53–3.23	[33,36,39]
	Liver infarction	0.04–1.61	[32,36]
	Liver failure	0.08–3.23	[36,38]
Transcatheter arterial treatments	Catheter dislocation/migration	N/A	
	Hepatic arterial damage	16.02	[40]
	Segmental liver infarction	0.17	[41]
	Bile leakage and biloma	0.85–0.87	[41,42]
	Ischemic biliopathy	5.13	[43]
	Cholecystitis	0.30	[41]
	Abscess formation	0.22–1.28	[41,44]
	Liver failure	0.26–13.38	[41,45]
Transjugular Intrahepatic Portosystemic Shunt	Hemorrhagic complications	2.06	[46]
	Bile duct injury	1.37–5.00	[47,48]
	TIPS site infection	3.33–4.39	[46]
	Shunt stenosis	31.11–46.66	[49–51]
	Shunt occlusion	8.88–12.22	[52]
	Hemobilia	1.03–1.37	[46,47]
	Segmental liver infarction	0.26	[46]
	Liver failure	N/A	
Endoscopic Retrograde Cholangiopancreatography	Hemorrhagic complications	1.34–16.98	[53,54]
	Infections	1.44–3.77	[53,54]
	Stent misplacement	4.14–6.51	[55,56]
Percutaneous Transhepatic Cholangiography	Hemorrhagic complications	2.50–6.9	[57]
	Bile leakage/biloma	0.77–28.70	[57]
	Cholangitis	4.61–26.3	[57]

Footnote: N/A: not available, * The provided data is derived from a single case report and a literature review. The actual incidence of this condition may differ based on variations in patient demographics and the surgical techniques employed. ** Between the years 1991 and 2020, a total of 67 cases were reported [58]. However, a precise frequency was not identified.*** Especially affecting the peripheral branches of the biliary ducts.

radiological investigation challenging.

US can identify cystic-like lesions and reveal a range of findings from well-circumscribed collections in the liver parenchyma to large loculated fluid collections throughout the abdomen. Sensitivity of US in the detection of intra-abdominal bile collections is estimated to be 70 % [69,85,87]. CT can offer a precise localization of the biloma and detailed imaging of the surrounding structures but it may need to be complemented by contrast-enhanced MRI for a definitive diagnosis [88]. Biloma after radiofrequency ablation can present a "mural nodule in cyst" pattern on contrast-enhanced portal venous phase CT and axial fat-saturated T2-weighted MRI, typically several months post-treatment [89]. The mural nodule, which lacks enhancement, represents the treated tumor and necrotic tissue, while the cyst is filled with bile. This pattern arises from bile accumulation at the boundary between ablated and non-ablated tissue, eventually dissecting this interface. US or CT-guided sampling of the biloma followed by laboratory analysis might be necessary to confirm the diagnosis when previous imaging and clinical findings are inconclusive. MRI, including MRCP, can further delineate the characteristics of a biloma and bile leaks with sensitivity ranging from 53–63 % and a specificity between 51–66 %, indicating moderate diagnostic accuracy [90]. Gadolinium ethoxybenzyl (Gd-EOB-DTPA)-enhanced MRCP is also used for non-invasive diagnosis (Fig. 3), improving the accuracy metrics, offering a sensitivity of 76–82 % and a specificity consistently at 100 % [85,87,90,91]. Invasive imaging techniques such as endoscopic retrograde cholangiopancreatography (ERCP) and percutaneous transhepatic cholangiography can provide further guidance on management. They not only point out the location and severity of the injury but also enable interventions like stent placement or sphincterotomy [92]. These interventions aid in enhancing bile flow, draining bilomas, and decompressing the biliary system, thereby promoting healing [93].

5. Biliary strictures

Benign biliary strictures predominantly stem from iatrogenic causes, such as cholecystectomy, post-liver transplant, partial hepatectomy, hepaticojejunostomy, and exposure to chemotherapy or radiation. Injury to the common bile duct during laparoscopic or open cholecystectomy contributes to the majority of iatrogenic bile duct injuries, despite the overall incidence of benign biliary strictures post-cholecystectomy being relatively low (0.2–0.7 %) [94]. These strictures, commonly occurring in the common hepatic or common bile ducts due to inadvertent ligation, may be identified during surgery or manifest postoperatively as obstructive jaundice or peritonitis. Distinctly, biliary strictures following orthotopic liver transplant are characterized by either proximal stricture at the anastomosis level or peripheral stricture due to arterial flow impairment, resulting in ischemic cholangiopathy [95].

US exhibits high sensitivity (approximately 100 %) in detecting intrahepatic biliary dilation and the obstruction level but is less effective in identifying strictures or masses [94]. Multiphase contrast-enhanced CT, a valuable diagnostic tool in the evaluation of biliary strictures, reveals benign strictures with distinctive features such as smooth contours, regular wall edges, and limited extent of narrowing, offering a clear differentiation from the complex and irregular characteristics typical of malignant strictures. [96]. As a highly accurate imaging modality, MRCP is extensively utilized for evaluating biliary obstructions, achieving diagnostic sensitivity of 98 % although the accuracy of MRCP in differentiating various types of biliary strictures can vary from 30 % to 100 % [94,97–100]. For fibrotic strictures, MRCP typically shows a gradual narrowing, regular borders, and involvement of a short section of the biliary tract [101–103]. By combining both MRI and MRCP for differentiating benign from malignant strictures, studies have shown sensitivity values between 82.3 % and 95.6 %, specificity values ranging from 91.3 % to 93.8 %, and an overall accuracy between 89 % and 94.5 % [104,105].

6. Cholecystitis and gallbladder perforation

During invasive procedures in proximity to the gallbladder fossa, complications such as cholecystitis or gallbladder perforation may inadvertently arise. Acute acalculous cholecystitis (AAC) is characterized by acute inflammation of the gallbladder in the absence of lithiasis. [106]. A key factor in the development of AAC is the injury caused by

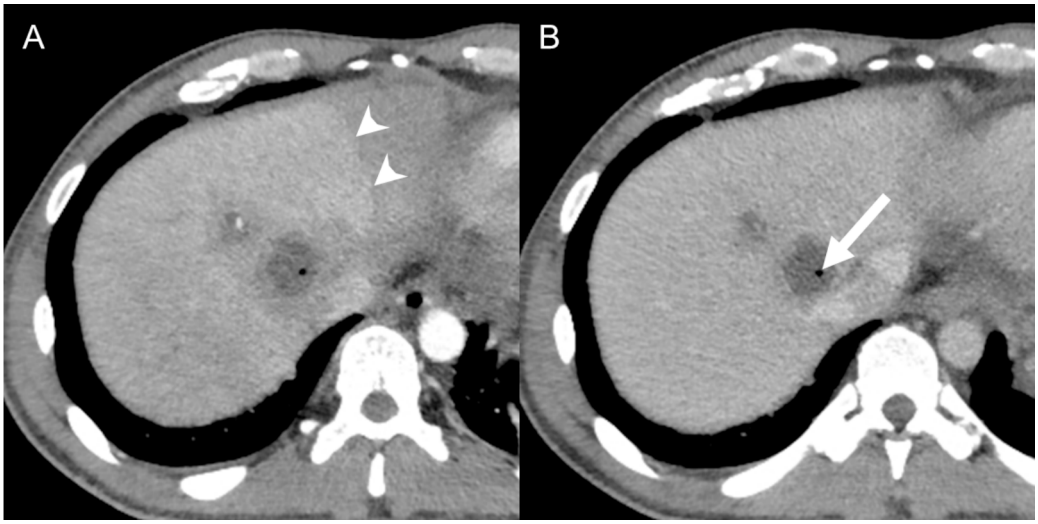

Fig. 2. 42-year-old man with acute pancreatitis who underwent endoscopic retrograde cholangiopancreatography. Contrast-enhanced CT on hepatic arterial (A) and portal venous (B) phases show a hypodense hepatic abscess with targetoid appearance and inner air microbubbles (arrow). Note the wedge-shaped area of hyperenhancement in the right hepatic lobe on the hepatic arterial phase (arrowheads in A).

Fig. 3. 74-year-old man with persistent biliary output from subhepatic drainage after cholecystectomy. Axial T2-weighted sequence (A) demonstrates a round, fluid containing observation. Hepatobiliary phase images acquired at 30 min (B) and 35 min (C) after the injection of gadoxetate disodium shows a progressive filling of the contrast agent (arrows) within the observation, due to a biliary leak from the hepatic hilum, allowing the diagnosis of biloma.

ischemia–reperfusion. Given that the gallbladder artery is a terminal artery, inadequate blood flow often results in ischemic necrosis of the gallbladder wall. The diagnosis of AAC is often made through clinical symptoms such as pain in the right upper abdomen, a positive Murphy's sign, and a raised temperature [107]. Acute cholecystitis can escalate, leading to dire complications such as gallbladder perforation, a medical emergency which can lead to a peritoneal infection. Contributing factors to gallbladder injury and perforation encompass inflammation, decreased gallbladder motility, prior surgical adhesions, or the presence of a percutaneous cholecystostomy catheter during ablation [96].

The US diagnostic criteria of AAC contain a positive Murphy sign, where the pain is induced by probe pressure on the gallbladder area, lack of gallstone, gallbladder enlargement (transverse diameter more than 5 cm and vertical diameter more than 8 cm), and a thickened gallbladder wall (more than 3.5 mm), known as a "double-wall" sign. US can also detect the presence of peritoneal effusion and the occurrence of echoes in the gallbladder. Sensitivity and specificity of US can range between 30 % and 100 % [107]. CT scans can be used to confirm AAC diagnosis when US results are inconclusive. CT diagnostic criteria involve a lack of gallstones, wall thickening (more than 3 mm), pericholecystic fat stranding, and signs of more severe conditions like gangrenous cholecystitis or gallbladder perforations. MRCP can visualize the pancreatic-biliary ductal system without contrast agents, making it non-invasive and safe. While ERCP is another diagnostic option, its invasive nature combined with a higher risk of pancreatitis causes MRCP to be often favored, especially in post-intervention or critical patients [108].

For gallbladder perforation, US manifestations overlap with AAC with a sensitivity of 31.5 % [109,110]. The 'sonographic-hole' sign, defined as the direct visualization of a defect in the gallbladder wall, serves as a highly specific indicator of gallbladder perforation and is detectable across US, CT, and MRI imaging modalities [111]. In some cases of gallbladder perforation, adhesions of the omentum to the adjacent gallbladder can obscure the gallbladder wall, making it challenging to assess the location and dimensions of the perforations using conventional US. CEUS, on the other hand, enhances the visibility of the gallbladder wall during the early arterial phase, presenting it as a "hyperechoic line", showing hyperenhanement compared to the surrounding liver parenchyma [112]. A recent case series demonstrated that small vessel slow flow perfusion Doppler imaging effectively identifies perforated gallbladders, highlighting features like unclear gallbladder walls and perfusion defects [113]. Enhancing this method with spectral analysis measurements such as Peak Systolic Velocity (PSV) and Resistive Index (RI) could provide more detailed insights into gallbladder conditions. This combined approach offers both visual and quantitative data, potentially improving the diagnosis of gallbladder perforations, though further clinical validation is needed. CT stands as the most sensitive diagnostic tool for gallbladder perforation. The findings encompass changes in gallbladder, pericholecystic, and other organs. Gallbladder changes involve enhancement and thickening of the gallbladder wall except for gangrenous gallbladder, wall defects, and intramural gas and collections (Fig. 4). Pericholecystic changes include fat stranding, fluid collections, biloma, and extra-luminal stones. Other organs may show pericholecystic liver enhancement, liver abscesses, portal vein thrombosis, pneumoperitoneum, intestinal wall thickening, and ascites [110]. MRI is a rarely used modality for suspected gallbladder perforations. There are a few case reports of gallbladder perforation utilized MRI which showed wall defect and intraluminal haematoma on post-contrast imaging and a loculated collection in the

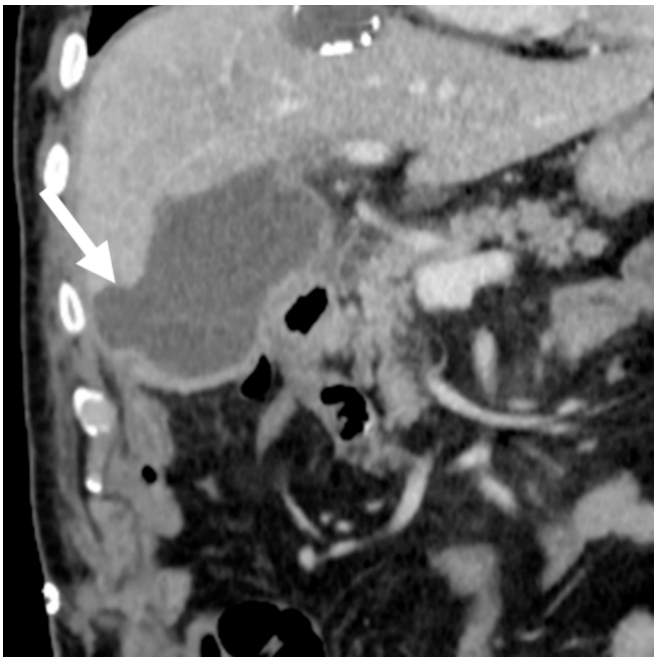

Fig. 4. 70-year-old woman with injury of the gallbladder wall after thermal ablation of hepatic metastasis in the right liver lobe. Coronal contrast-enhanced CT on portal venous phase demonstrates a distended gallbladder with wall thickening and irregular wall defects (arrow), suggestive of perforation.

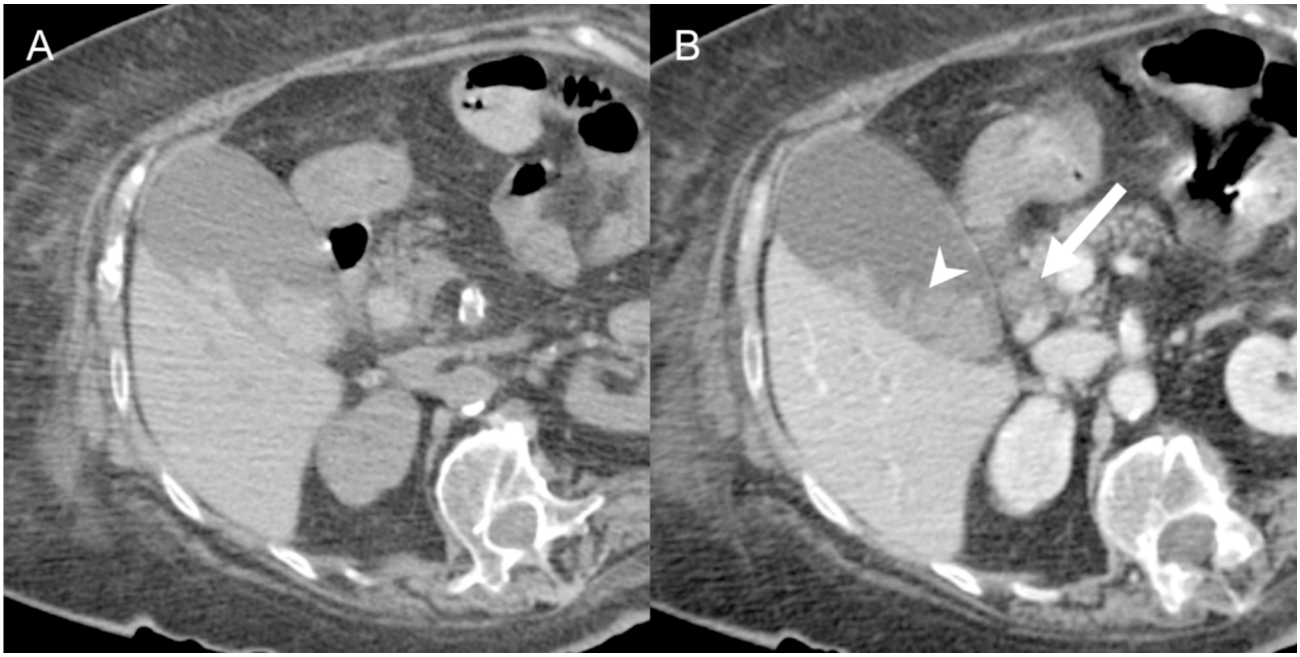

Fig. 5. 74-year-old woman with hemobilia after endoscopic retrograde cholangiopancreatography. Pre-contrast (A) and contrast-enhanced CT on portal venous phase (B) show dilatation of the main bile duct with hyperdense material in the common bile duct (arrow) and in the gallbladder lumen (arrowhead) consistent with blood. No evidence of active bleeding is observed.

pericholecystic region [114,115].

7. Hemobilia

This condition is characterized by the extravasation of blood into the bile ducts, often resulting from iatrogenic injuries, including complications following ERCP [116]. It is particularly prevalent in instances of interventions on the caudate lobe in deeper regions of the liver, where there exists a heightened risk of simultaneous damage to vessels and bile ducts [34]. Patients with hemobilia can exhibit symptoms such as jaundice, melena, and abdominal pain [13].

On US, clots can be seen as floating hyperechoic material within anechoic biliary lumen, however detecting clots, especially smaller ones, within the bile ducts is challenging using US due to the clots' diminished echogenicity and their tendency to adhere to ductal walls in case of self-limiting hemobilia. In active hemobilia, the injection of a US contrast agent can demonstrate contrast agent bubbles filling the gallbladder lumen [117]. In emergency situations, CT angiography is the first-line modality for detecting hemobilia. It offers accurate identification and pinpointing of the bleed's origin, allowing for prompt and decisive intervention [116]. Scattered hyperdensities can be observed within bile ducts on a pre-contrast CT scan (Fig. 5). Additionally, enhancement of the ductal walls post-contrast injection may point to a cholangitic process, potentially initiated by the persistent hemorrhagic stimulus on the ductal walls [117]. MRI with MRCP can demonstrate intrabiliary filling defects with fluid–fluid level, mass-like, or cast-like appearance with mixed signal intensity on T2-weighted images consistent with blood products in various stages of breakdown and high signal intensity on T1-weighted images could be in favor of hemobilia in the proper clinical setting and history of recent iatrogenic or accidental trauma. Active extravasation of contrast material into the lumen of the biliary tract, can be demonstrated by dynamic MRI, with findings similar to those with contrast enhanced CT. Subtraction imaging techniques help distinguish between other hyperintense duct obstructions, such as gallstones or sediment, and genuine blood flow [116,118].

8. Fistula formation

Fistula can form at various locations depending on the type of hepatic intervention. Biliocutaneous, enterobiliary, bronchobiliary, biliopleural, arteriovenous, and arterioportal fistulae are reported as complications of hepatic interventions, especially after biopsy, ablation, and cholecystectomy [17,18,25,32,38]. The clinical presentation of biliary fistulas is usually with abdominal pain, jaundice, and raised inflammatory markers in the immediate postoperative period or productive bilious coughs in bronchobiliary fistula [119]. Several factors may contribute to the formation of fistulas, including the size and location of the ablated liver tumor, the proximity of vital structures, the experience of the operator, and the technique used during the procedure [119]. Inadequate ablative margins, incomplete coagulation of tissues, or excessive energy delivery can increase the risk of fistula formation [119].

US has shown high diagnostic accuracy in patients with arteriovenous fistulae, with a sensitivity of 83.3 % and a specificity of 90.7 % [120]. On Doppler ultrasound, arteriovenous fistulas display a low-impedance, bidirectional blood flow within the portal vein [121]. US and contrast-enhanced CT are useful for the diagnosis of associated biliary dilation, pneumobilia, biloma, and collection or visualization of the fistulous tract [122]. MRI and MRCP, with T2-weighted sequences, identifies hyperintense fistulous tracts, while the hepatobiliary phase with hepatobiliary specific agents including Gadobenate dimeglumine (Gd-BOPTA), and Gd-EOB-DTPA play role as good substitutions of hepatic iminodiacetic acid (HIDA) scan to show biliary agent leak into adjacent organ [123,124]. ERCP and cutaneous cholangiography are particularly effective for visualizing contrast extravasation from the biliary system into other organs such as lung, gastrointestinal tract, and vascular structure the management is conservative for most fistula with an external drainage catheter, endoscopic sphincterotomy and/or stent placement meanwhile embolization for biliovascular fistula is recommended [124,125].

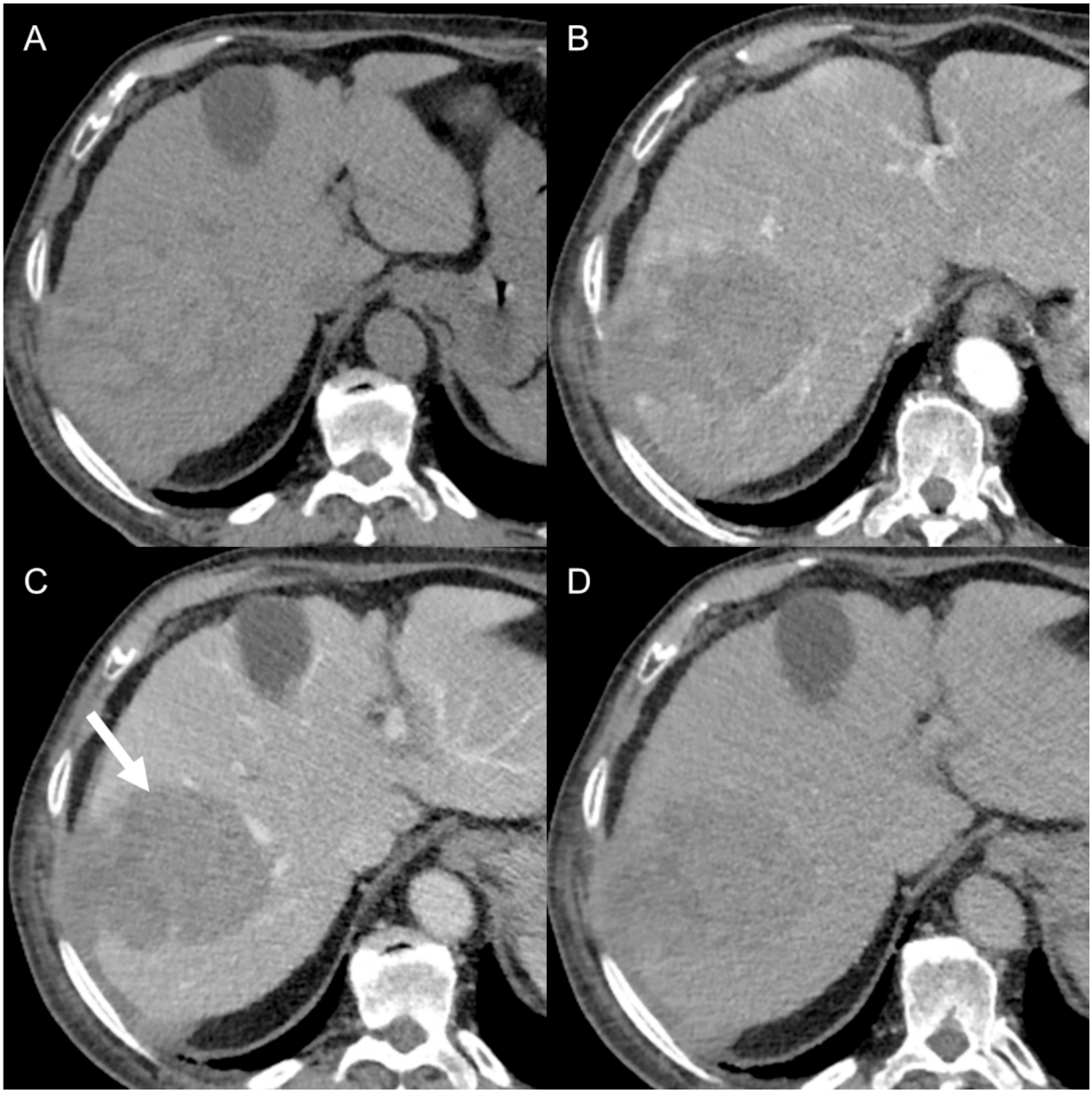

Fig. 6. 80-year-old man with hepatic hematoma after percutaneous liver biopsy performed in the liver parenchyma for suspected autoimmune hepatitis. CT images on pre-contrast (A), hepatic arterial (B), portal venous (C), and delayed phases show a large intraparenchymal hematoma (arrow) extended to the liver capsule in the right hepatic lobe without evidence of active bleeding.

9. Hemorrhagic complications

Intraperitoneal bleeding is one of the most prevalent serious complications following various interventions underscoring the importance of vigilant monitoring [126]. This complication is often related to direct mechanical injury, and when lesions situated adjacent to large vessels are treated. Patients with cirrhosis are at elevated risk, with the main cause being the coagulopathy brought about by hepatic dysfunction [34].

US is typically the first-line diagnostic tool for suspected post-interventional hemorrhage. Hematomas on US often appear avascular echogenic in acute phase and will show different levels of internal echo in the first month [127]. CEUS excels as a tool for prompt detection and facilitates the planning of subsequent treatment strategies [128]. The characteristic feature of active bleeding along the needle track observed in CEUS is the linear spillage of microbubbles during the vascular phase into the peritoneal cavities. In instances of hemoperitoneum, CEUS is distinguished by a jet-like leakage of contrast agents from various pathological sources into the perihepatic peritoneal space. For subcapsular hematomas, CEUS reveals unenhanced areas within the liver parenchyma, which are marked by their convex margins [117]. On CT scan, the hematoma manifests as a biconvex or enlarging intraparenchymal lesion, typically superficial at the device entry point, and high-density values between 45–70 Hounsfield Units (HU) in precontrast images without any enhancement on post contrast phases (Fig. 6). However, in the presence of active bleeding there is extravasation of contrast material or increased enhancement of hematoma (Fig. 7) ranging between 85 and 370 HU [129,130]. MRI distinguishes between active bleeding, hematomas, and other hepatic lesions with sensitivity of 94 % and specificity of 82–89 % [131]. However, MRI's utility is limited by its longer scanning times and less accessibility compared to US and CT in emergent settings. Hematoma appears notably hyperintense on

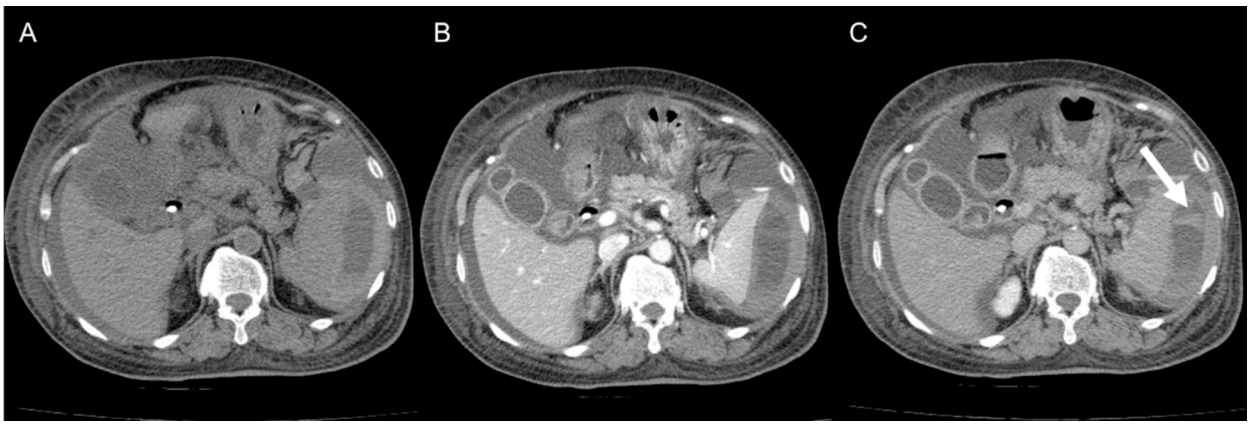

Fig. 7. 50-year-old man with bleeding from a distal branch of the splenic artery occurring after endoscopic retrograde cholangiopancreatography performed for stenting of infiltrating cholangiocarcinoma in the common bile duct. CT images on pre-contrast (A), portal venous (B), and delayed (C) phases demonstrate a perisplenic hematoma with progressive contrast extravasation (arrow).

T2-weighted MRI at its onset. It typically presents with regular borders, adopting shapes such as biconvex, biconcave, or "quarter-moon," which varies based on whether it is situated peripherally or more towards the center of the liver [132]. The active bleeding exhibited isointense signals on both T1 and T2-weighted images, suggesting the presence of intracellular oxyhemoglobin characteristic of an acute hemorrhage [133].

10. Thromboses

Vascular thrombosis represents a serious complication that can arise following various medical interventions. This complication may manifest several hours after a procedure. In patients with hepatocellular carcinoma, it's essential to differentiate post-interventional thrombosis from tumor thrombosis or disease progression. Depending on the vessel involved, thromboses can range from minor to major complications, with smaller-caliber vessels that exhibit diminished flow due to previous treatments or existing conditions being more susceptible [13].

Acute arterial thrombosis in US presents as an intraluminal hyperechoic spot due to fresh thrombus formation in hepatic arteries close to 100 % sensitivity, devoid of inner flow on color Doppler [134]. Subacute arterial thrombosis demonstrates reduced echogenicity compared to acute arterial thrombosis, indicating clot maturation [134]. Contrast-enhanced CT, as a secondary diagnostic approach, is essential if hepatic Doppler ultrasound indicates abnormalities or encounters technical challenges. In contrast-enhanced CT, the diagnosis of hepatic artery thrombosis is suggested by the absence of contrast uptake in the hepatic artery, which is indicative of impaired or halted arterial blood flow. This imaging modality demonstrates a sensitivity and specificity of 100 % and 97 %, respectively, for identifying hepatic artery thrombosis and stenosis, compared to invasive angiography, which is typically reserved for therapeutic interventions [135]. In MRI, acute arterial thrombosis presents as isointense on T1-weighted imaging, with heterogeneity on T2-weighted imaging. As the clot ages, MRI characteristics transition, with variable intensity on both T1 and T2-weighted imaging [136].

Acute venous thrombosis detects a distinct, hyperechoic thrombus in the portal or hepatic vein, absent of inner flow on color doppler, and subacute venous thrombosis echogenicity diminishes over time, making it harder to differentiate from surrounding tissue [13]. On CEUS, portal vein thrombosis is identified by a lack of filling in the portal vein [134]. The thrombus appears less defined with time, but vascular congestion may persist. Contrast-enhanced CT reveals an intraluminal defect in the portal vein or hepatic veins (Fig. 8), often accompanied by segmental enhancement of the nearby liver tissue. This is likely due to a compensatory increase in local arterial blood flow. Conversely, hepatic vein thrombosis is most identifiable during the portal or equilibrium phase of contrast-enhanced CT, commonly linked with a wedge-shaped area of the liver exhibiting reduced enhancement due to vascular congestion [13,137]. Acute venous thrombus appears as a clear intraluminal defect on MRI. Over time, MRI characteristics of the venous thrombus shift, showing increased heterogeneity [13,134,136,138].

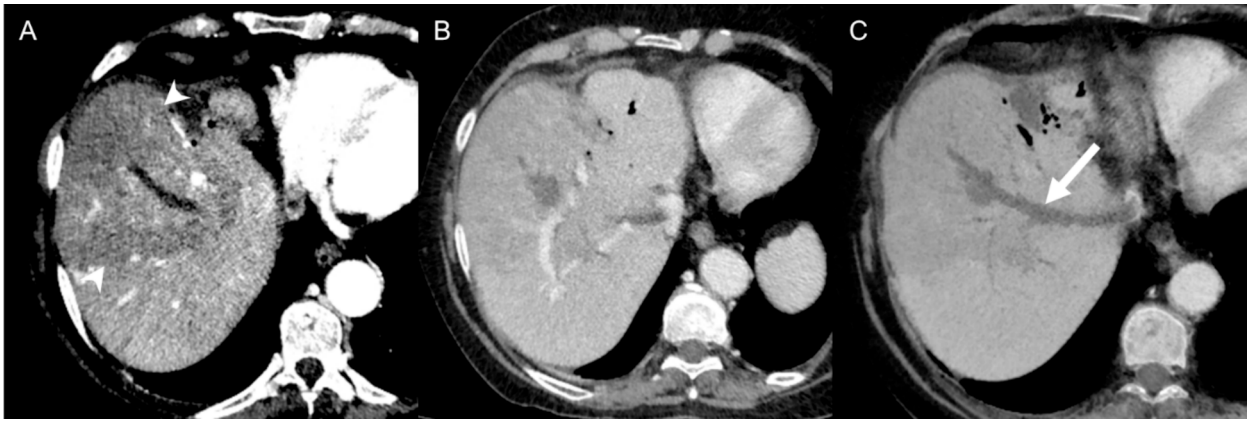

Fig. 8. 78-year-old woman with hepatocellular carcinoma treated with percutaneous ablation. Post-interventional contrast-enhanced CT on hepatic arterial (A), portal venous (B) phase and MinIP reconstruction (C) show a new nontumoral thrombosis of the right hepatic vein (arrow in C) with segmental hypoenhancement in the drained area better visible on the hepatic arterial phase (arrowheads in A).

11. Pseudoaneurysms

Pseudoaneurysms after laparoscopic cholecystectomy are clinically significant, with 81 % of patients showing symptoms like gastrointestinal bleeding and abdominal pain within the first eight weeks which affect 74 % and 61 % of patients, respectively [14]. About 28 % of cases also present with bile duct damage or bile leakage, and one-third of pseudoaneurysms occur even after uncomplicated laparoscopic cholecystectomy [14]. Therefore, any patient with abdominal pain or bleeding signs post laparoscopic cholecystectomy should be evaluated for a pseudoaneurysm. The most commonly implicated arteries include the right hepatic artery (70 %), the cystic artery (19 %), or a combination of both (3 %), primarily due to iatrogenic damage to a hepatic artery branch [14].

The sensitivity of US can vary based on the size of the pseudoaneurysm, and it might have limitations in detecting small pseudoaneurysms. Upon US examination, a pseudoaneurysm might resemble an anechoic area, akin to a cyst formation. The diagnostic process is significantly facilitated by the use of color Doppler imaging, which reveals the characteristic yin-yang sign, indicative of turbulent flow within the lesion [14]. During the arterial phase of a contrast-enhanced CT study, pseudoaneurysms are discernible as small, well-delineated hyperdense nodules within the location area of previous intervention [139]. CT angiography stands as the most dependable non-invasive technique for detecting pseudoaneurysms. It can provide the pseudoaneurysm's location and size, thrombosed pseudoaneurysms, abnormal vessels, and anatomical variations. Traditional angiography, although invasive and demanding a skilled interventional radiologist, shows a sensitivity of 90 %, pinpointing the exact location and size of the pseudoaneurysm, uncovering the bleeding source, and can seamlessly transition from a diagnostic to a therapeutic procedure. MRI can distinguish between a blood clot and a gallstone in cases of obstructive jaundice for instance [14]. On MRI, acute blood clots (less than 1 week old) typically show as isointense or slightly hypointense on T1-weighted images and hyperintense on T2-weighted images, while clots aged 1–6 weeks become hyperintense on both T1 and T2 images due to methemoglobin [140]. Clots older than 6 weeks appear hypointense on both T1 and T2 images because of hemosiderin [140]. Gallstones contrastingly exhibit variable signals; on T1-weighted images, cholesterol gallstones are typically hypointense and pigment gallstones hyperintense, whereas on T2-weighted images, gallstones are generally hypointense, though internal structures like fluid-filled clefts can appear hyperintense [141,142]. Monitoring the progression of the pseudoaneurysm's diameter is essential for determining the necessity of further interventions [143].

12. Liver infarction

Liver infarction is rare but significant complication, often prolonging hospital stays and limiting further treatments [144]. The liver's dual blood supply from the hepatic artery and portal vein typically protects it from infarction, but compromise can lead to necrosis and secondary infections, potentially causing abscesses and sepsis. The risk factors following transcatheter arterial treatments include non-selective injections, large masses, and repeated procedures [145,146,42]. Infarctions are more common in treatments for liver metastases than hepatocellular carcinoma, likely due to the absence of cirrhosis formerly [147]. Patients without cirrhosis face higher risks of locoregional complications, unlike those with cirrhosis who benefit from a protective vascular network against infarction [144,148].

On both conventional and Doppler ultrasound, liver infarctions

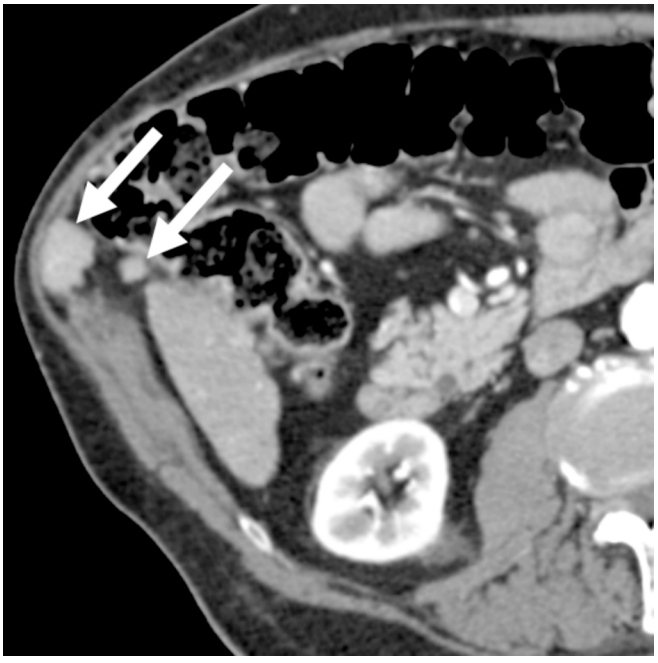

Fig. 10. 78-year-old man with cirrhosis and hepatocellular carcinoma proved at surgical resection. Follow-up contrast enhanced CT demonstrates multiple enhancing tumor nodules (arrows) due to tumor seeding in the perihepatic abdominal fat and in the abdominal wall.

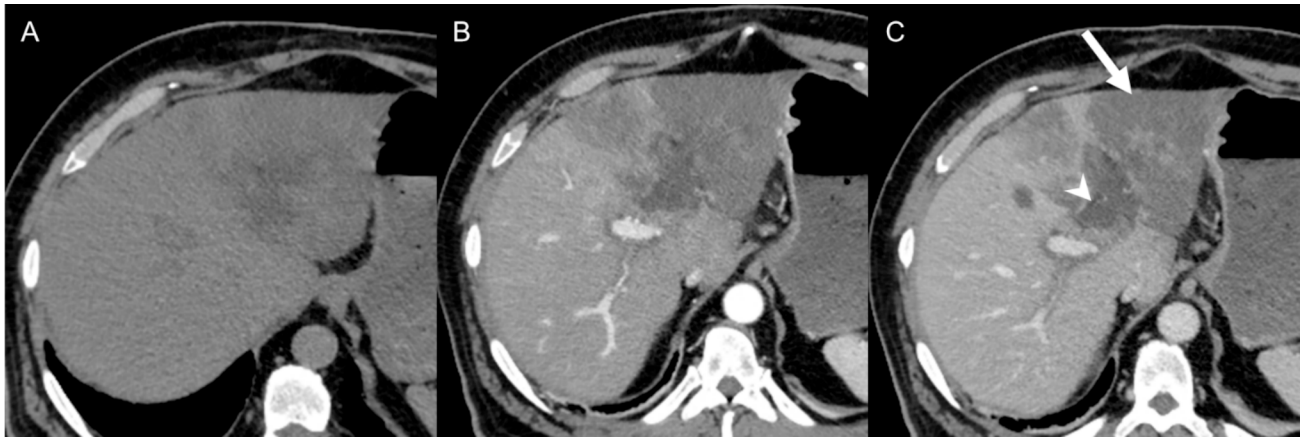

Fig. 9. 68-year-old man with hepatic infarction after cholecystectomy for gallbladder carcinoma. Pre-contrast (A), hepatic arterial (B), and portal venous (C) phases show a large wedge-shaped area of hepatic infarction (arrow) in the left liver lobe associated with thrombosis of the left portal vein (arrowhead) and lack of opacification of the intrahepatic branches of the left hepatic artery.

manifest as hypoechoic, nonvascular areas. These hypoechoic zones, located at the periphery of the liver, often exhibit internal echogenic bands indicating liver infarcts. This distinctive "bright band" sign can be a valuable diagnostic indicator to distinguish infarctions from abscesses [149]. On CT, infarcted liver areas typically manifest as hypodense regions that fail to enhance post contrast administration (Fig. 9) [144]. The CT findings are closely aligned with the gross pathological changes seen in liver infarction. Typically, liver infarcts can be distinguished as clear-cut regions, markedly different from the surrounding tissue and are extended in a wedge shape towards the liver's edge [150]. On MRI, liver infarctions demonstrate wedge shape hypointensity on T1-weighted sequences and hyperintensity on T2-weighted sequences without signal loss on opposed-phase images excluding focal fatty liver. Normal vessels coursing through these areas confirm the lack of mass effect. [144,151].

13. Tumor seeding

Tumor seeding, a rare but serious complication of percutaneous interventions, involves the accidental implantation of tumor cells along the intervention path, leading to potential metastasis [11]. This dissemination of cells can initiate new tumor growth at different sites, complicating the clinical situation and possibly diminishing the benefits of the intervention [60]. The risk of seeding is heightened during biopsy compared to therapeutic procedures like ablation [152]. In a retrospective study, no wall seeding was observed for ablations only, while the rate was 0.13 % for biopsies only and 2.70 % when both procedures were conducted [37]. To reduce the probability of needle seeding, the coaxial biopsy method is reported as a safer method than other approaches because it allows multiple samples of the lesion to be taken with just one puncture [153].

Tumor seeding closely mimics the primary tumor's radiographic appearance as an enhancing, irregular soft tissue structures along the track of the device (Fig. 10). However, post-ablation inflammatory changes often serve as a confounding factor, as these too can exhibit similar imaging features. Biopsy stands as the definitive means of differentiation, offering histopathological insights [60].

14. TIPS stenosis or occlusion

TIPS stenosis emerges as a significant complication, predominantly resulting from fibrous tissue infiltration into the endograft, thereby narrowing the lumen [116 154]. Previous studies showed that within two years post-TIPS creation, between 29–85 % of patients faced TIPS dysfunction depending the type of stent (bare or covered) [155,156]. In instances of recurrent thrombotic TIPS occlusion, it is imperative to exclude hypercoagulopathy, given its prevalence in patients recommended for TIPS, thereby predisposing them to thrombosis. Nevertheless, acute shunt thrombosis is noted in less than 5 % of TIPS insertions [157]. Particularly with bare metal stents, acute TIPS occlusion is frequently attributed to the formation of biliary-venous fistulas, considering the thrombogenic nature of bile [157]. Though the introduction of covered stents has bolstered patency, stenosis still affects 8–21 % of patients one-year post-TIPS insertion [155,158].

On post-implementation of the TIPS, Doppler imaging visually represents the blood flow in the stent, portal, and hepatic venous systems [158]. Detecting sonographic abnormalities necessitates a subsequent TIPS angiography accompanied by portal pressure measurements [158]. Some studies proposed a one-year post-TIPS angiographic assessment for patients to ascertain portal decompression and shunt patency [158]. Stent velocities below 90 cm/s in doppler indicate roughly 50 % stent stenosis, and those under 50–60 cm/s suggest potential failure. Conversely, exceeding 250 cm/s suggests significant lumen reduction, akin to high-grade arterial stenosis. Doppler velocities below 50 cm/s or above 250 cm/s within the stent have over 90 % sensitivity and specificity in pinpointing stent malfunctions [159]. Using color Doppler ultrasound to detect TIPS dysfunction with covered metal stents showed a satisfactory sensitivity of 82 %, but its specificity was only 58 % [160]. To enhance diagnostic accuracy, researchers have explored the use of CT, for evaluating TIPS (Fig. 11). This approach has demonstrated a sensitivity of 92 % and a specificity of 77 % in identifying hemodynamically significant stenosis [161]. MRI is limited for evaluating stenosis in TIPS stents due to artifacts caused by the stent materials [162].

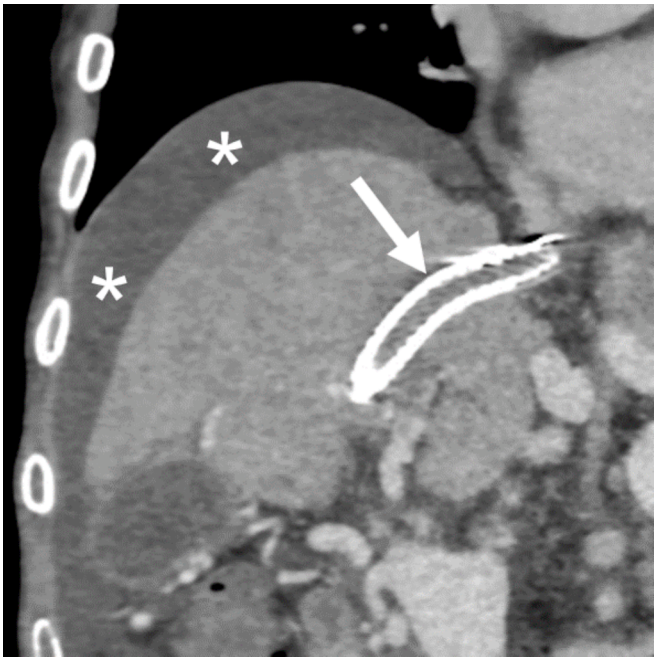

Fig. 11. 68-year-old man with occluded TIPS. Coronal contrast-enhanced CT image on portal venous phase demonstrates lack of enhancement within the TIPS (arrow) consistent with TIPS occlusion. Note the presence of ascites (*) as complication of portal hypertension.

15. Advances in imaging

Emerging imaging technologies, such as dual-energy CT (DECT) and photon-counting CT (PCCT), have recently shown promise in enhancing diagnostic capabilities [163,164]. These tools offer higher spatial resolution and improved conspicuity of liver lesions, even at smaller sizes [165]. The possibilities to perform virtual monoenergetic imaging and material decomposition reconstructions, significantly enhance tissue characterization, improve contrast enhancement, and reduce beam hardening artifacts [166,167]. These advancements allow for more precise differentiation of tissue properties by utilizing the unique responses of different materials at varying energy levels. Despite their potential, there is a need for further research to establish the specific applications and accuracy of these advanced imaging modalities in the management of post-interventional complications.

16. Conclusion

Understanding the radiological findings associated with post-intervention complications is crucial for promptly identifying primary complications that may arise following a procedure. This awareness facilitates early and targeted intervention, thereby mitigating the risk of adverse outcomes. The US serves as a valuable diagnostic instrument during treatment and acts as a surveillance tool, providing real-time imaging and monitoring of the treated area. This role could be augmented using color Doppler and CEUS. The CT scan with multiphase contrast study continues to be the preferred tool in emergency settings, offering a comprehensive view of the internal structures and aiding in

the immediate diagnosis of complications. Dynamic MRI, MRCP and specific hepatobiliary contrast agents offering detailed images of the liver and surrounding tissues, thereby contributing to the nuanced understanding of the patient's condition.

Declaration of generative AI and AI-assisted technologies in the writing process

During the preparation of this work, the authors used ChatGPT/OpenAI for checking grammar and sentence structure. After using this tool, the authors reviewed and edited the content and take full responsibility for the content of the publication.

Funding

Roberto Cannella: co-funding by the European Union - FESR or FSE, PON Research and Innovation 2014-2020 - DM 1062/2021.

CRediT authorship contribution statement

Faezeh Khorasanizadeh: Writing – review & editing, Writing – original draft, Visualization, Supervision, Project administration. **Narges Azizi:** Writing – original draft, Visualization. **Roberto Cannella:** Writing – review & editing, Writing – original draft, Visualization, Supervision, Conceptualization. **Giuseppe Brancatelli:** Writing – review & editing, Supervision.

Declaration of competing interest

The authors declare the following financial interests/personal relationships which may be considered as potential competing interests: Roberto Cannella: support for attending meetings from Bracco and Bayer; research collaboration with Siemens Healthcare.

References

[1] A. Pepe, F. Crimì, F. Vernuccio, G. Cabrelle, A. Lupi, C. Zanon, et al., Medical radiology current progress, Diagnostics [internet]. 13 (14) (2023).
[2] K.K. Brock, S.R. Chen, R.A. Sheth, J.H. Siewerdsen, Imaging in interventional radiology: 2043 and beyond, Radiology 308 (1) (2023) e230146.
[3] A. Posa, P. Barbieri, G. Mazza, A. Tanzilli, L. Natale, E. Sala, et al., Technological advancements in interventional oncology, Diagnostics. 13 (2) (2023) 228.
[4] I. Patel, S. Rehman, S. McKay, D. Bartlett, D. Mirza, Use of near-infrared fluorescence techniques in minimally invasive surgery for colorectal liver metastases, J. Clin. Med. 12 (17) (2023) 5536.
[5] V.F. Schmidt, O. Dietrich, P.M. Kazmierczak, M. Seidensticker, J. Ricke, M. Armbruster, Optimized visualization of focal liver lesions and vascular structures in real-time T1-weighted gradient echo sequences for magnetic resonance-guided liver procedures, Diagn Interv Radiol. 29 (1) (2023) 128–137.
[6] A.B. Chowdhury, K.J. Mehta, Liver biopsy for assessment of chronic liver diseases: a synopsis, Clin. Exp. Med. 23 (2) (2023) 273–285.
[7] T.L. Sutton, L.H. Wong, B.S. Walker, E.N. Dewey, R. Eil, C.D. Lopez, et al., Hepatectomy is associated with improved oncologic outcomes in recurrent colorectal liver metastases: a propensity-matched analysis, Surgery 173 (6) (2023) 1314–1321.
[8] K. Vidyadharan, R. KembaiShanmugam, G. Ayyasamy, S. Thandayuthapani, Early versus delayed laparoscopic cholecystectomy in uncomplicated biliary colic: an observational study, Laparoscopic, Endoscopic Robotic Surgery. 6 (2) (2023) 69–72.
[9] Norero B, Bosch J, Berzigotti A, Rodrigues SG. Transjugular intrahepatic portosystemic shunt in patients with hepatocellular carcinoma: A systematic review. United European Gastroenterology Journal. 2023;n/a(n/a).
[10] C.L. Hallemeier, N. Sharma, C. Anker, J.E. Selfridge, P. Lee, S. Jabbour, et al., American radium society appropriate use criteria for the use of liver-directed therapies for nonsurgical management of liver metastases: systematic review and guidelines, Cancer 129 (20) (2023) 3193–3212.
[11] M. Ahmed, L. Solbiati, C.L. Brace, D.J. Breen, M.R. Callstrom, J.W. Charboneau, et al., Image-guided tumor ablation: standardization of terminology and reporting criteria–a 10-year update, J Vasc Interv Radiol. 25 (11) (2014), 1691 705.e4.
[12] Gavriilidis P, Catena F, de'Angelis G, de'Angelis N. Consequences of the spilled gallstones during laparoscopic cholecystectomy: a systematic review. World Journal of Emergency Surgery. 2022;17(1):57.
[13] F. De Muzio, C. Cutolo, F. Dell'Aversana, F. Grassi, L. Ravo, M. Ferrante, et al., Complications after thermal ablation of hepatocellular carcinoma and liver metastases: imaging findings, Diagnostics (basel) 12 (5) (2022).
[14] C. Lampropoulos, G. Markopoulos, S. Tsochatzis, A. Bellou, T. Amanatidis, D. Kehagias, et al., Symptomatic pseudoaneurysms following laparoscopic cholecystectomy: focus on an unusual and dangerous complication, J Minim Access Surg. 17 (4) (2021) 450–457.
[15] M. Midia, D. Odedra, A. Shuster, R. Midia, J. Muir, Predictors of bleeding complications following percutaneous image-guided liver biopsy: a scoping review, Diagn Interv Radiol. 25 (1) (2019) 71–80.
[16] H.B. Thomaides-Brears, N. Alkhouri, D. Allende, M. Harisinghani, M. Noureddin, N.S. Reau, et al., Incidence of complications from percutaneous biopsy in chronic liver disease: a systematic review and meta-analysis, Dig Dis Sci. 67 (7) (2022) 3366–3394.
[17] Norman Oneil M. Complications of Liver Biopsy - Risk Factors, Management and Recommendations. In: Hirokazu T, editor. Liver Biopsy. Rijeka: IntechOpen; 2011. p. Ch. 25.
[18] K. Okuda, H. Musha, Y. Nakajima, K. Takayasu, Y. Suzuki, M. Morita, et al., Frequency of intrahepatic arteriovenous fistula as a sequela to percutaneous needle puncture of the liver, Gastroenterology 74 (6) (1978) 1204–1207.
[19] T. Sano, K. Shimada, Y. Sakamoto, J. Yamamoto, S. Yamasaki, T. Kosuge, One hundred two consecutive hepatobiliary resections for perihilar cholangiocarcinoma with zero mortality, Ann Surg. 244 (2) (2006) 240–247.
[20] R.A. Schroeder, C.E. Marroquin, B.P. Bute, S. Khuri, W.G. Henderson, P.C. Kuo, Predictive indices of morbidity and mortality after liver resection, Ann Surg. 243 (3) (2006) 373–379.
[21] P.C. Simmonds, J.N. Primrose, J.L. Colquitt, O.J. Garden, G.J. Poston, M. Rees, Surgical resection of hepatic metastases from colorectal cancer: a systematic review of published studies, Br J Cancer. 94 (7) (2006) 982–999.
[22] H. Takata, A. Hirakata, J. Ueda, T. Yokoyama, H. Maruyama, N. Taniai, et al., Prediction of portal vein thrombosis after hepatectomy for hepatocellular carcinoma, Langenbecks Arch. Surg. 406 (3) (2021) 781–789.
[23] N. Yoshida, S. Yamazaki, M. Masamichi, Y. Okamura, T. Takayama, Prospective validation to prevent symptomatic portal vein thrombosis after liver resection, World J Hepatol. 14 (5) (2022) 1016–1024.
[24] M. Radunovic, R. Lazovic, N. Popovic, M. Magdelinic, M. Bulajic, L. Radunovic, et al., Complications of laparoscopic cholecystectomy: our experience from a retrospective analysis, Open Access Maced J Med Sci. 4 (4) (2016) 641–646.
[25] N. Acar, T. Acar, Y. Sür, H. Bağ, H. Kar, Y. Yılmaz Bozok, et al., Is subtotal cholecystectomy safe and feasible? Short- and long-term results, J. Hepatobiliary Pancreat. Sci. 28 (3) (2021) 263–271.
[26] V. Dev, D. Shah, F. Gaw, A.T. Lefor, Gastric outlet obstruction secondary to post cholecystectomy biloma: case report and review of the literature, Jsls. 2 (2) (1998) 185–188.
[27] B. Pottakkat, R. Vijayahari, A. Prakash, R.K. Singh, A. Behari, A. Kumar, et al., Incidence, pattern and management of bile duct injuries during cholecystectomy: experience from a single center, Dig Surg. 27 (5) (2010) 375–379.
[28] W.M. Tay, Y.J. Toh, V.G. Shelat, C.W. Huey, S.P. Junnarkar, W. Woon, et al., Subtotal cholecystectomy: early and long-term outcomes, Surg. Endosc. 34 (10) (2020) 4536–4542.
[29] C. Dewhurst, R.A. Kane, J.N. Mhuircheartaigh, O. Brook, M. Sun, B. Siewert, Complication rate of ultrasound-guided percutaneous cholecystostomy in patients with coagulopathy, AJR Am J Roentgenol. 199 (6) (2012) W753–W760.
[30] H. Yamahata, M. Yabuta, M. Rahman, Retrospective comparison of clinical outcomes of ultrasound-guided percutaneous cholecystostomy in patients with and without coagulopathy: a single center's experience, Jpn J Radiol. 41 (9) (2023) 1015–1021.
[31] M.F. Byrne, P. Suhocki, R.M. Mitchell, T.N. Pappas, H.L. Stiffler, P.S. Jowell, et al., Percutaneous cholecystostomy in patients with acute cholecystitis: experience of 45 patients at a US referral center, J Am Coll Surg. 197 (2) (2003) 206–211.
[32] T. Livraghi, L. Solbiati, M.F. Meloni, G.S. Gazelle, E.F. Halpern, S.N. Goldberg, Treatment of focal liver tumors with percutaneous radio-frequency ablation: complications encountered in a multicenter study, Radiology 226 (2) (2003) 441–451.
[33] M. Dollinger, L.P. Beyer, M. Haimerl, C. Niessen, E.M. Jung, F. Zeman, et al., Adverse effects of irreversible electroporation of malignant liver tumors under CT fluoroscopic guidance: a single-center experience, Diagn Interv Radiol. 21 (6) (2015) 471–475.
[34] H. Rhim, K.H. Yoon, J.M. Lee, Y. Cho, J.S. Cho, S.H. Kim, et al., Major complications after radio-frequency thermal ablation of hepatic tumors: spectrum of imaging findings, Radiographics 23 (1) (2003), pp. 123–34; discussion 34–6.
[35] T. Shibata, Y. Yamamoto, N. Yamamoto, Y. Maetani, T. Shibata, I. Ikai, et al., Cholangitis and liver abscess after percutaneous ablation therapy for liver tumors: incidence and risk factors, J Vasc Interv Radiol. 14 (12) (2003) 1535–1542.
[36] X. Li, Y. Zhang, X. Wang, H. Zeng, L. Zhou, G. Huang, et al., Predicting infectious complications after percutaneous thermal ablation of liver malignancies: a 12-year single-center experience, Radiology 308 (2) (2023) e223091.
[37] J.L. Szpakowski, T.E. Drasin, L.L. Lyon, Rate of seeding with biopsies and ablations of hepatocellular carcinoma: a retrospective cohort study, Hepatol Commun. 1 (9) (2017) 841–851.
[38] P. Schullian, E. Johnston, G. Laimer, D. Putzer, G. Eberle, A. Amann, et al., Frequency and risk factors for major complications after stereotactic radiofrequency ablation of liver tumors in 1235 ablation sessions: a 15-year experience, Eur Radiol. 31 (5) (2021) 3042–3052.
[39] I. Kurilova, A. Bendet, E.N. Petre, F.E. Boas, E. Kaye, M. Gonen, et al., Factors associated with local tumor control and complications after thermal ablation of colorectal cancer liver metastases: a 15-year retrospective cohort study, Clin. Colorectal Cancer 20 (2) (2021) e82–e95.

[40] N. Maeda, K. Osuga, K. Mikami, H. Higashihara, H. Onishi, Y. Nakaya, et al., Angiographic evaluation of hepatic arterial damage after transarterial chemoembolization for hepatocellular carcinoma, Radiat Med. 26 (4) (2008) 206–212.
[41] I. Sakamoto, N. Aso, K. Nagaoki, Y. Matsuoka, M. Uetani, K. Ashizawa, et al., Complications associated with transcatheter arterial embolization for hepatic tumors, Radiographics 18 (3) (1998) 605–619.
[42] J.W. Chung, J.H. Park, J.K. Han, B.I. Choi, M.C. Han, H.S. Lee, et al., Hepatic tumors: predisposing factors for complications of transcatheter oily chemoembolization, Radiology 198 (1) (1996) 33–40.
[43] S. Nakada, M.A. Allard, M. Lewin, S. Awad, N. Dahbi, H. Nitta, et al., Ischemic cholangiopathy following transcatheter arterial chemoembolization for recurrent hepatocellular carcinoma after hepatectomy: an underestimated and devastating complication, J Gastrointest Surg. 24 (11) (2020) 2517–2525.
[44] M. Arslan, S. Degirmencioglu, Liver abscesses after transcatheter arterial embolization, J Int Med Res. 47 (3) (2019) 1124–1130.
[45] Y.S. Huang, J.H. Chiang, J.C. Wu, F.Y. Chang, S.D. Lee, Risk of hepatic failure after transcatheter arterial chemoembolization for hepatocellular carcinoma: predictive value of the monoethylglycinexylidide test, Am J Gastroenterol. 97 (5) (2002) 1223–1227.
[46] D. Bettinger, M. Schultheiss, T. Boettler, M. Muljono, R. Thimme, M. Rössle, Procedural and shunt-related complications and mortality of the transjugular intrahepatic portosystemic shunt (TIPSS), Aliment Pharmacol Ther. 44 (10) (2016) 1051–1061.
[47] X. Yin, L. Gu, M. Zhang, Q. Yin, J. Xiao, Y. Wang, et al., Covered TIPS procedure-related major complications: incidence, management and outcome from a single center, Front. Med. 9 (2022).
[48] G. Mamone, M. Milazzo, A. Di Piazza, S. Caruso, V. Carollo, G. Gentile, et al., Transjugular intrahepatic portosystemic shunt (TIPS) complications: what diagnostic radiologists should know, Abdom Radiol (NY). 47 (12) (2022) 4254–4270.
[49] C.D. Lind, T.W. Malisch, W.K. Chong, W.O. Richards, C.W. Pinson, S.G. Meranze, et al., Incidence of shunt occlusion or stenosis following transjugular intrahepatic portosystemic shunt placement, Gastroenterology 106 (5) (1994) 1277–1283.
[50] Z.J. Haskal, M.J. Pentecost, M.C. Soulen, R.D. Shlansky-Goldberg, R.A. Baum, C. Cope, Transjugular intrahepatic portosystemic shunt stenosis and revision: early and midterm results, AJR Am J Roentgenol. 163 (2) (1994) 439–444.
[51] J.M. LaBerge, K.A. Somberg, J.R. Lake, R.L. Gordon, R.K. Kerlan Jr., N.L. Ascher, et al., Two-year outcome following transjugular intrahepatic portosystemic shunt for variceal bleeding: results in 90 patients, Gastroenterology 108 (4) (1995) 1143–1151.
[52] A.J. Stanley, R. Jalan, E.H. Forrest, D.N. Redhead, P.C. Hayes, Longterm follow up of transjugular intrahepatic portosystemic stent shunt (TIPSS) for the treatment of portal hypertension: results in 130 patients, Gut 39 (3) (1996) 479–485.
[53] A. Andriulli, S. Loperfido, G. Napolitano, G. Niro, M.R. Valvano, F. Spirito, et al., Incidence rates of post-ERCP complications: a systematic survey of prospective studies, Am J Gastroenterol. 102 (8) (2007) 1781–1788.
[54] K. Nathaniel, Y. Daniel, A.-M. Fray, M. Ghassan, C. Derrick, V. Shivakumar, Outcomes and risk factors for ERCP-related complications in a predominantly black urban population, BMJ Open Gastroenterol. 7 (1) (2020) e000462.
[55] M.A. Taj, S. Ghazanfar, S. Qureshi, M. Zubair, S.K. Niaz, M.S. Quraishy, Plastic stent migration in ERCP; a tertiary care experience, J Pak Med Assoc. 69 (8) (2019) 1099–1102.
[56] A. Kale, S. Sundaram, M. Aggarwal, S. Giri, H. Darak, G. Jain, et al., Predictors of proximal migration of straight biliary plastic stents, Indian J Gastroenterol (2023).
[57] A.S. Turan, S. Jenniskens, J.M. Martens, M.J.C.M. Rutten, L.S.F. Yo, M.J.L. van Strijen, et al., Complications of percutaneous transhepatic cholangiography and biliary drainage, a multicenter observational study, Abdominal Radiology. 47 (9) (2022) 3338–3344.
[58] S.M.J. Taghavi, M. Jaya Kumar, R. Damodaran Prabha, H. Puhalla, C. Sommerville, Cystic artery pseudoaneurysm: current review of aetiology, presentation, and management, Surg Res Pract. 2021 (2021) 4492206.
[59] J.-J. Yoo, T.K. Lee, D.-S. Kyoung, M.-A. Park, S.G. Kim, Y.S. Kim, A population-based study of pyogenic liver abscess in Korea: incidence, mortality and temporal trends during 2007–2017, Liver Int. 41 (11) (2021) 2747–2758.
[60] N.I. Sainani, D.A. Gervais, P.R. Mueller, R.S. Arellano, Imaging after percutaneous radiofrequency ablation of hepatic tumors: part 2, Abnormal Findings. AJR Am J Roentgenol. 200 (1) (2013) 194–204.
[61] D. Choi, H.K. Lim, M.J. Kim, S.J. Kim, S.H. Kim, W.J. Lee, et al., Liver abscess after percutaneous radiofrequency ablation for hepatocellular carcinomas: frequency and risk factors, AJR Am J Roentgenol. 184 (6) (2005) 1860–1867.
[62] H.N. Lee, D. Hyun, Complications related to transarterial treatment of hepatocellular carcinoma: a comprehensive review, Korean J Radiol. 24 (3) (2023) 204–223.
[63] S. Woo, J.W. Chung, S. Hur, S.M. Joo, H.C. Kim, H.J. Jae, et al., Liver abscess after transarterial chemoembolization in patients with bilioenteric anastomosis: frequency and risk factors, AJR Am J Roentgenol. 200 (6) (2013) 1370–1377.
[64] A.A. Malik, S.U. Bari, K.A. Rouf, K.A. Wani, Pyogenic liver abscess: changing patterns in approach, World J Gastrointest Surg. 2 (12) (2010) 395–401.
[65] S. Malekzadeh, L. Widmer, F. Salahshour, B. Egger, M. Ronot, H.C. Thoeny, Typical imaging finding of hepatic infections: a pictorial essay, Abdom Radiol (NY). 46 (2) (2021) 544–561.
[66] O. Catalano, F. Sandomenico, M.M. Raso, A. Siani, Low mechanical index contrast-enhanced sonographic findings of pyogenic hepatic abscesses, AJR Am J Roentgenol. 182 (2) (2004) 447–450.
[67] D. Giambelluca, F. Panzuto, E. Giambelluca, M. Midiri, The, "double target sign" in liver abscess, Abdom Radiol (NY). 43 (10) (2018) 2885–2886.
[68] R.B. Jeffrey Jr., C.S. Tolentino, F.C. Chang, M.P. Federle, CT of small pyogenic hepatic abscesses: the cluster sign, AJR Am J Roentgenol. 151 (3) (1988) 487–489.
[69] S. Thomas, K. Jahangir, Noninvasive imaging of the biliary system relevant to percutaneous interventions, Semin Intervent Radiol. 33 (4) (2016) 277–282.
[70] M.H. Park, H. Rhim, Y.S. Kim, D. Choi, H.K. Lim, W.J. Lee, Spectrum of CT findings after radiofrequency ablation of hepatic tumors, Radiographics 28 (2) (2008), pp. 379–90; discussion 90–2.
[71] S.Y. Huang, A. Philip, M.D. Richter, S. Gupta, M.L. Lessne, C.Y. Kim, Prevention and management of infectious complications of percutaneous interventions, Semin Intervent Radiol. 32 (2) (2015) 78–88.
[72] J.W. Melamed, E.K. Paulson, M.A. Kliewer, Sonographic appearance of oxidized cellulose (Surgicel): pitfall in the diagnosis of postoperative abscess, J Ultrasound Med. 14 (1) (1995) 27–30.
[73] T. Okabayashi, Y. Shima, T. Sumiyoshi, K. Sui, J. Iwata, S. Morita, et al., Incidence and risk factors of cholangitis after hepaticojejunostomy, J Gastrointest Surg. 22 (4) (2018) 676–683.
[74] H. Gomi, T. Takada, T.L. Hwang, K. Akazawa, R. Mori, I. Endo, et al., Updated comprehensive epidemiology, microbiology, and outcomes among patients with acute cholangitis, J Hepatobiliary Pancreat Sci. 24 (6) (2017) 310–318.
[75] J. Schneider, A. Hapfelmeier, S. Thöres, A. Obermeier, C. Schulz, D. Pförringer, et al., Mortality risk for acute cholangitis (MAC): a risk prediction model for in-hospital mortality in patients with acute cholangitis, BMC Gastroenterol. 16 (1) (2016) 15.
[76] Y. Kihara, H. Yokomizo, The clinical features of late postoperative cholangitis following pancreaticoduodenectomy brought on by conditions other than cancer recurrence: a single-center retrospective study, BMC Surg. 22 (1) (2022) 301.
[77] S. Touzani, A. El Bouazzaoui, F. Bouyarmane, K. Faraj, N. Houari, B. Boukatta, et al., Factors associated with mortality in severe acute cholangitis in a moroccan intensive care unit: a retrospective analysis of 140 cases, Gastroenterol Res Pract. 2021 (2021) 4583493.
[78] K. Minaga, M. Kitano, H. Imai, K. Yamao, K. Kamata, T. Miyata, et al., Urgent endoscopic ultrasound-guided choledochoduodenostomy for acute obstructive suppurative cholangitis-induced sepsis, World J. Gastroenterol. 22 (16) (2016) 4264.
[79] P. Mosler, Diagnosis and management of acute cholangitis, Curr. Gastroenterol. Rep. 13 (2) (2011) 166–172.
[80] A. Sokal, A. Sauvanet, B. Fantin, V. de Lastours, Acute cholangitis: diagnosis and management, J. Visc. Surg. 156 (6) (2019) 515–525.
[81] G. Umefune, H. Kogure, T. Hamada, H. Isayama, K. Ishigaki, K. Takagi, et al., Procalcitonin is a useful biomarker to predict severe acute cholangitis: a single-center prospective study, J. Gastroenterol. 52 (6) (2017) 734–745.
[82] S.W. Kim, H.C. Shin, H.C. Kim, M.J. Hong, I.Y. Kim, Diagnostic performance of multidetector CT for acute cholangitis: evaluation of a CT scoring method, Br. J. Radiol. 85 (1014) (2012) 770–777.
[83] A. Singh, H.S. Mann, C.L. Thukral, N.R. Singh, Diagnostic accuracy of MRCP as compared to ultrasound/CT in patients with obstructive jaundice, J Clin Diagn Res. 8 (3) (2014) 103–107.
[84] F. Mehmood, A. Khalid, S. Frager, Perihepatic biloma in a non-cirrhotic patient after transjugular intrahepatic portosystemic shunt (TIPS), Cureus. 14 (3) (2022) e23399.
[85] J. Balfour, A. Ewing, Hepatic, StatPearls Publishing, Treasure Island (FL), Biloma, 2022 2022..
[86] M. Zhu, G. Li, Y. Chen, G. Gong, W. Guo, Clinical features and treatment of hepatic abscesses with biloma formation after transcatheter arterial chemoembolization, Arab J. Gastroenterology. 23 (1) (2022) 32–38.
[87] A. Copelan, L. Bahoura, F. Tardy, M. Kirsch, F. Sokhandon, B. Kapoor, Etiology, diagnosis, and management of bilomas: a current update, Tech Vasc Interv Radiol. 18 (4) (2015) 236–243.
[88] M. Di Martino, I. Mora-Guzmán, V.V. Jodra, A.S. Dehesa, D.M. García, R.C. Ruiz, et al., How to predict postoperative complications after early laparoscopic cholecystectomy for acute cholecystitis: the chole-risk score, J. Gastrointest. Surg. 25 (11) (2021) 2814–2822.
[89] Y.S. Kim, H. Rhim, H.K. Lim, D. Choi, M.W. Lee, M.J. Park, Coagulation necrosis induced by radiofrequency ablation in the liver: histopathologic and radiologic review of usual to extremely rare changes, Radiographics 31 (2) (2011) 377–390.
[90] de'Angelis N, Catena F, Memeo R, Coccolini F, Martínez-Pérez A, Romeo OM, et al. 2020 WSES guidelines for the detection and management of bile duct injury during cholecystectomy. World J Emerg Surg. 2021;16(1):30.
[91] M. Kantarcı, B. Pirimoglu, N. Karabulut, U. Bayraktutan, H. Ogul, G. Ozturk, et al., Non-invasive detection of biliary leaks using Gd-EOB-DTPA-enhanced MR cholangiography: comparison with T2-weighted MR cholangiography, Eur Radiol. 23 (10) (2013) 2713–2722.
[92] C.M. Thompson, N.E. Saad, R.R. Quazi, M.D. Darcy, D.D. Picus, C.O. Menias, Management of iatrogenic bile duct injuries: role of the interventional radiologist, Radiographics 33 (1) (2013) 117–134.
[93] A.M. Nikpour, R.J. Knebel, D. Cheng, Diagnosis and management of postoperative biliary leaks, Semin Intervent Radiol. 33 (4) (2016) 307–312.
[94] A. Altman, S.M. Zangan, Benign biliary strictures, Semin Intervent Radiol. 33 (4) (2016) 297–306.

[95] A. Singh, A. Gelrud, B. Agarwal, Biliary strictures: diagnostic considerations and approach, Gastroenterol Rep (oxf). 3 (1) (2015) 22–31.
[96] S.H. Choi, J.K. Han, J.M. Lee, K.H. Lee, S.H. Kim, J.Y. Lee, et al., Differentiating malignant from benign common bile duct stricture with multiphasic helical CT, Radiology 236 (1) (2005) 178–183.
[97] M. Suthar, S. Purohit, V. Bhargav, P. Goyal, Role of MRCP in differentiation of benign and malignant causes of biliary obstruction, J Clin Diagn Res. 9(11):Tc08-12 (2015).
[98] M.J. Kim, D.G. Mitchell, K. Ito, E.K. Outwater, Biliary dilatation: differentiation of benign from malignant causes–value of adding conventional MR imaging to MR cholangiopancreatography, Radiology 214 (1) (2000) 173–181.
[99] H.S. Heinzow, S. Kammerer, C. Rammes, J. Wessling, D. Domagk, T. Meister, Comparative analysis of ERCP, IDUS, EUS and CT in predicting malignant bile duct strictures, World J Gastroenterol. 20 (30) (2014) 10495–10503.
[100] B.S. Kapoor, G. Mauri, J.M. Lorenz, Management of biliary strictures: state-of-the-art review, Radiology 289 (3) (2018) 590–603.
[101] N. Shabanikia, A. Adibi, S. Ebrahimian, Diagnostic accuracy of magnetic resonance cholangiopancreatography to detect benign and malignant biliary strictures, Adv Biomed Res. 10 (2021) 38.
[102] J.A. Soto, E.K. Yucel, M.A. Barish, R. Chuttani, J.T. Ferrucci, MR cholangiopancreatography after unsuccessful or incomplete ERCP, Radiology 199 (1) (1996) 91–98.
[103] J. Romagnuolo, M. Bardou, E. Rahme, L. Joseph, C. Reinhold, A.N. Barkun, Magnetic resonance cholangiopancreatography: a meta-analysis of test performance in suspected biliary disease, Ann Intern Med. 139 (7) (2003) 547–557.
[104] M. Bilgin, H. Toprak, M. Burgazli, S.S. Bilgin, R. Chasan, A. Erdogan, et al., Diagnostic value of dynamic contrast-enhanced magnetic resonance imaging in the evaluation of the biliary obstruction, ScientificWorldJournal 2012 (2012) 731089.
[105] L. Zhong, Q.Y. Yao, L. Li, J.R. Xu, Imaging diagnosis of pancreato-biliary diseases: a control study, World J Gastroenterol. 9 (12) (2003) 2824–2827.
[106] P.E. Stevens, N.A. Harrison, D.J. Rainford, Acute acalculous cholecystitis in acute renal failure, Intensive Care Med. 14 (4) (1988) 411–416.
[107] Y. Fu, L. Pang, W. Dai, S. Wu, J. Kong, Advances in the study of acute acalculous cholecystitis: a comprehensive review, Dig. Dis. 40 (4) (2021) 468–478.
[108] O.J. O'Connor, M.M. Maher, Imaging of Cholecystitis, Am. J. Roentgenol. 196 (4) (2011) W367–W374.
[109] C.M. Peterson, M.M. McNamara, I.R. Kamel, W.B. Al-Refaie, H. Arif-Tiwari, B. D. Cash, et al., ACR Appropriateness Criteria(®) Right Upper Quadrant Pain, J Am Coll Radiol. 16 (5s) (2019) S235–S243.
[110] M.M. Harraz, A.H. Abouissa, Role of MSCT in the diagnosis of perforated gall bladder (a retrospective study), Egypt. J. Radiol. Nucl. Med. 51 (1) (2020) 4.
[111] Boruah DK, Sanyal S, Sharma BK, Boruah DR. Comparative Evaluation of Ultrasonography and Cross-sectional Imaging in Determining Gall Bladder Perforation in Accordance to Niemeier's Classification. J Clin Diagn Res. 2016;10 (8):Tc15-8.
[112] S. Tang, Y. Wang, Y. Wang, Contrast-enhanced ultrasonography to diagnose gallbladder perforation, Am. J. Emerg. Med. 31 (8) (2013) 1240–1243.
[113] M.U. Aziz, M.L. Robbin, Improved detection of gallbladder perforation using ultrasound small vessel slow flow "perfusion" imaging, J Ultrasound Med. 41 (2) (2022) 511–518.
[114] Y.C. Wong, L.J. Wang, C.J. Chen, MRI of an isolated traumatic perforation of the gallbladder, J Comput Assist Tomogr. 24 (4) (2000) 657–658.
[115] B. Sood, M. Jain, N. Khandelwal, P. Singh, S. Suri, MRI of perforated gall bladder, Australas. Radiol. 46 (4) (2002) 438–440.
[116] A. Parvinian, J.G. Fletcher, A.C. Storm, S.K. Venkatesh, J.L. Fidler, A. R. Khandelwal, Challenges in diagnosis and management of hemobilia, Radiographics 41 (3) (2021) 802–813.
[117] G. Francica, M.F. Meloni, L. Riccardi, F. Giangregorio, E. Caturelli, F. Terracciano, et al., Role of contrast-enhanced ultrasound in the detection of complications after ultrasound-guided liver interventional procedures, J Ultrasound Med. 40 (8) (2021) 1665–1673.
[118] N.K. Lee, S. Kim, J.W. Lee, S.H. Lee, D.H. Kang, D.U. Kim, et al., MR appearance of normal and abnormal bile: correlation with imaging and endoscopic finding, Eur J Radiol. 76 (2) (2010) 211–221.
[119] M. Krokidis, G. Orgera, M. Rossi, M. Matteoli, A. Hatzidakis, Interventional radiology in the management of benign biliary stenoses, biliary leaks and fistulas: a pictorial review, Insights Imaging. 4 (1) (2013) 77–84.
[120] Y.Y. Li, Y.Y. Duan, G.Z. Yan, F.Q. Lv, W. Cao, T.S. Cao, et al., Application of ultrasonography in the diagnosis and treatment tracing of hepatocellular carcinoma-associated arteriovenous fistulas, Liver Int. 27 (6) (2007) 869–875.
[121] B. Cao, K. Tian, H. Zhou, C. Li, D. Liu, Y. Tan, Hepatic arterioportal fistulas: a retrospective analysis of 97 cases, J Clin Transl Hepatol. 10 (4) (2022) 620–626.
[122] C.K. Chou, Computed tomography demonstration of cholecystogastric fistula, Radiol Case Rep. 11 (2) (2016) 70–73.
[123] K.L. Gage, S. Deshmukh, K.J. Macura, I.R. Kamel, A. Zaheer, MRI of perianal fistulas: bridging the radiological-surgical divide, Abdom Imaging. 38 (5) (2013) 1033–1042.
[124] G.Q. Liao, H. Wang, G.Y. Zhu, K.B. Zhu, F.X. Lv, S. Tai, Management of acquired bronchobiliary fistula: a systematic literature review of 68 cases published in 30 years, World J Gastroenterol. 17 (33) (2011) 3842–3849.
[125] T.R. Khalid, V.J. Casillas, B.M. Montalvo, R. Centeno, J.U. Levi, Using MR cholangiopancreatography to evaluate iatrogenic bile duct injury, Am. J. Roentgenol. 177 (6) (2001) 1347–1352.
[126] F. Izzo, V. Granata, R. Grassi, R. Fusco, R. Palaia, P. Delrio, et al., Radiofrequency ablation and microwave ablation in liver tumors: an update, Oncologist. 24 (10) (2019) e990–e1005.
[127] D.S. Bhangle, K. Sun, J.S. Wu, Imaging features of soft tissue tumor mimickers: a pictorial essay, Indian J Radiol Imaging. 32 (3) (2022) 381–394.
[128] Z. Sparchez, T. Mocan, R. Craciun, M. Sparchez, C. Nolsøe, Contrast enhancement for ultrasound-guided interventions: when to use it and what to expect? Ultrasonography. 41 (2) (2022) 263–278.
[129] M. Akahane, H. Koga, N. Kato, H. Yamada, K. Uozumi, R. Tateishi, et al., Complications of percutaneous radiofrequency ablation for hepato-cellular carcinoma: imaging spectrum and management, Radiographics 25 (Suppl 1) (2005) S57–S68.
[130] M. Lubner, C. Menias, C. Rucker, S. Bhalla, C.M. Peterson, L. Wang, et al., Blood in the belly: CT findings of hemoperitoneum, Radiographics 27 (1) (2007) 109–125.
[131] A.P. Matos, F. Velloni, M. Ramalho, M. AlObaidy, A. Rajapaksha, R.C. Semelka, Focal liver lesions: practical magnetic resonance imaging approach, World J Hepatol. 7 (16) (2015) 1987–2008.
[132] A. Manenti, L. Roncati, G. Manco, A. Farinetti, F. Coppi, Hepatic hematoma: a challenging, emergency disease, Surgery Open Digestive Advance. 10 (2023) 100084.
[133] T. Allam, R. Sweis, P.S. Sander, MRI spot sign: gadolinium contrast extravasation in an expanding intracerebral hematoma on MRI, Radiol Case Rep. 14 (5) (2019) 535–537.
[134] C.E. Brookmeyer, S. Bhatt, E.K. Fishman, S. Sheth, Multimodality imaging after liver transplant: top 10 important complications, Radiographics 42 (3) (2022) 702–721.
[135] J. Dumortier, C. Besch, L. Moga, A. Coilly, F. Conti, C. Corpechot, et al., Non-invasive diagnosis and follow-up in liver transplantation, Clin. Res. Hepatol. Gastroenterol. 46 (1) (2022) 101774.
[136] R.C. Jha, S.S. Khera, A.D. Kalaria, Portal vein thrombosis: imaging the spectrum of disease with an emphasis on MRI features, Am. J. Roentgenol. 211 (1) (2018) 14–24.
[137] S.L. Novick, E.K. Fishman, Portal vein thrombosis: spectrum of helical CT and CT angiographic findings, Abdom Imaging. 23 (5) (1998) 505–510.
[138] R. Cannella, A. Taibbi, G. Porrello, M. Dioguardi Burgio, G. Cabibbo, T. V. Bartolotta, Hepatocellular carcinoma with macrovascular invasion: multimodality imaging features for the diagnosis, Diagn Interv Radiol. 26 (6) (2020) 531–540.
[139] V. Sivakumar, 'Washing machine' and 'yin-yang' sign in popliteal pseudoaneurysm, QJM 114 (3) (2021) 212.
[140] R. Corti, J.I. Osende, Z.A. Fayad, J.T. Fallon, V. Fuster, G. Mizsei, et al., In vivo noninvasive detection and age definition of arterial thrombus by MRI, J Am Coll Cardiol. 39 (8) (2002) 1366–1373.
[141] Y.L. Chan, W.W. Lam, C. Metreweli, S.C. Chung, Detectability and appearance of bile duct calculus on MR imaging of the abdomen using axial T1- and T2-weighted sequences, Clin Radiol. 52 (5) (1997) 351–355.
[142] M. Ukaji, M. Ebara, Y. Tsuchiya, H. Kato, H. Fukuda, N. Sugiura, et al., Diagnosis of gallstone composition in magnetic resonance imaging: in vitro analysis, Eur J Radiol. 41 (1) (2002) 49–56.
[143] Y.S. Kim, H. Rhim, H.K. Lim, Imaging after radiofrequency ablation of hepatic tumors, Semin Ultrasound CT MR. 30 (2) (2009) 49–66.
[144] J. Joskin, T. de Baere, A. Auperin, L. Tselikas, B. Guiu, G. Farouil, et al., Predisposing factors of liver necrosis after transcatheter arterial chemoembolization in liver metastases from neuroendocrine tumor, Cardiovasc. Interv. Radiol. 38 (2) (2015) 372–380.
[145] I. Sakamoto, S. Iwanaga, K. Nagaoki, Y. Matsuoka, K. Ashizawa, M. Uetani, et al., Intrahepatic biloma formation (bile duct necrosis) after transcatheter arterial chemoembolization, AJR Am J Roentgenol. 181 (1) (2003) 79–87.
[146] J.S. Yu, K.W. Kim, M.G. Jeong, D.H. Lee, M.S. Park, S.W. Yoon, Predisposing factors of bile duct injury after transcatheter arterial chemoembolization (TACE) for hepatic malignancy, Cardiovasc Intervent Radiol. 25 (4) (2002) 270–274.
[147] J.S. Yu, K.W. Kim, M.S. Park, S.W. Yoon, Bile duct injuries leading to portal vein obliteration after transcatheter arterial chemoembolization in the liver: CT findings and initial observations, Radiology 221 (2) (2001) 429–436.
[148] H. Mayan, R. Kantor, U. Rimon, N. Golubev, Z. Heyman, E. Goshen, et al., Fatal liver infarction after transjugular intrahepatic portosystemic shunt procedure, Liver 21 (5) (2001) 361–364.
[149] G. Whang, S. Chopra, H. Tchelepi, "Bright band sign" a grayscale ultrasound finding in hepatic infarction, J Ultrasound Med. 38 (9) (2019) 2515–2520.
[150] D.D. Adler, G.M. Glazer, T.M. Silver, Computed tomography of liver infarction, AJR Am J Roentgenol. 142 (2) (1984) 315–318.
[151] J.A. Parra, L. Hernández, P. Muñoz, G. Blanco, R. Rodríguez-Álvarez, D.R. Vilar, et al., Detection of spleen, kidney and liver infarcts by abdominal computed tomography does not affect the outcome in patients with left-side infective endocarditis, Medicine (Baltimore) 97 (33) (2018) e11952.
[152] G. Cabibbo, A. Craxì, Needle track seeding following percutaneous procedures for hepatocellular carcinoma, World J Hepatol. 1 (1) (2009) 62–66.
[153] G. Francica, Needle track seeding after radiofrequency ablation for hepatocellular carcinoma: prevalence, impact, and management challenge, J Hepatocell Carcinoma. 4 (2017) 23–27.
[154] R. Cannella, L. Tselikas, F. Douane, F. Cauchy, P.E. Rautou, R. Duran, et al., Imaging-guided interventions modulating portal venous flow: evidence and controversies, JHEP Rep. 4 (7) (2022) 100484.

[155] A. Luca, R. Miraglia, S. Caruso, M. Milazzo, C. Sapere, L. Maruzzelli, et al., Short- and long-term effects of the transjugular intrahepatic portosystemic shunt on portal vein thrombosis in patients with cirrhosis, Gut 60 (6) (2011) 846–852.
[156] A. Di Giorgio, E. Nicastro, R. Agazzi, M. Colusso, L. D'Antiga, Long-term outcome of transjugular intrahepatic portosystemic shunt in children with portal hypertension, J Pediatr Gastroenterol Nutr. 70 (5) (2020) 615–622.
[157] P.V. Suhocki, M.P. Lungren, B. Kapoor, C.Y. Kim, Transjugular intrahepatic portosystemic shunt complications: prevention and management, Semin Intervent Radiol. 32 (2) (2015) 123–132.
[158] M. Darcy, Evaluation and management of transjugular intrahepatic portosystemic shunts, AJR Am J Roentgenol. 199 (4) (2012) 730–736.
[159] R.Y. Kanterman, M.D. Darcy, W.D. Middleton, K.M. Sterling, S.A. Teefey, T. K. Pilgram, Doppler sonography findings associated with transjugular intrahepatic portosystemic shunt malfunction, AJR Am J Roentgenol. 168 (2) (1997) 467–472.
[160] W. Manatsathit, H. Samant, P. Panjawatanan, A. Braseth, J. Suh, M. Esmadi, et al., Performance of ultrasound for detection of transjugular intrahepatic portosystemic shunt dysfunction: a meta-analysis, Abdom Radiol (NY). 44 (7) (2019) 2392–2402.
[161] S. Chopra, G.D. Dodd 3rd, K.N. Chintapalli, H. Rhim, C.E. Encarnacion, J. C. Palmaz, et al., Transjugular intrahepatic portosystemic shunt: accuracy of helical CT angiography in the detection of shunt abnormalities, Radiology 215 (1) (2000) 115–122.
[162] L.W. Bartels, C.J. Bakker, M.A. Viergever, Improved lumen visualization in metallic vascular implants by reducing RF artifacts, Magn Reson Med. 47 (1) (2002) 171–180.
[163] K.W. Shaqdan, A. Parakh, A.R. Kambadakone, D.V. Sahani, Role of dual energy CT to improve diagnosis of non-traumatic abdominal vascular emergencies, Abdom Radiol (NY). 44 (2) (2019) 406–421.
[164] D. Racine, V. Mergen, A. Viry, M. Eberhard, F. Becce, D.C. Rotzinger, et al., Photon-counting detector CT with quantum iterative reconstruction: impact on liver lesion detection and radiation dose reduction, Invest Radiol. 58 (4) (2023) 245–252.
[165] P.C. Douek, S. Boccalini, E.H.G. Oei, D.P. Cormode, A. Pourmorteza, L. Boussel, et al., Clinical applications of photon-counting CT: a review of pioneer studies and a glimpse into the future, Radiology 309 (1) (2023) e222432.
[166] M.H. Albrecht, T.J. Vogl, S.S. Martin, J.W. Nance, T.M. Duguay, J.L. Wichmann, et al., Review of clinical applications for virtual monoenergetic dual-energy CT, Radiology 293 (2) (2019) 260–271.
[167] T. Sartoretti, V. Mergen, K. Higashigaito, M. Eberhard, H. Alkadhi, A. Euler, Virtual noncontrast imaging of the liver using photon-counting detector computed tomography: a systematic phantom and patient study, Invest Radiol. 57 (7) (2022) 488–493.